Heliyon 10 (2024) e31429

Contents lists available at ScienceDirect

Heliyon

journal homepage: www.cell.com/heliyon

Research article

Preparation and characterization of novel nanostructured lipid carriers (NLC) and solid lipid nanoparticles (SLN) containing coenzyme Q10 as potent antioxidants and antityrosinase agents

Hoda Atapour-Mashhad [a,b], Zahra Tayarani-Najaran [c,d], Shiva Golmohammadzadeh [a,b,*]

[a] Nanotechnology Research Center, Pharmaceutical Technology Institute, Mashhad University of Medical Sciences, Mashhad, Iran
[b] Department of Pharmaceutics, Faculty of Pharmacy, Mashhad University of Medical Sciences, Mashhad, Iran
[c] Medical Toxicology Research Center, Mashhad University of Medical Sciences, Mashhad, Iran
[d] Targeted Drug Delivery Research Center, Pharmaceutical Technology Institute, Mashhad University of Medical Sciences, Mashhad, Iran

ARTICLE INFO

Keywords:
Co-Q10
Q10-NLC
Q10-SLN
Antioxidant
Antityrosinase

ABSTRACT

We developed novel and optimal Q10-NLC/SLN formulations as antioxidant and anti-tyrosinase agents. The formulations were analyzed for particle size, morphology, entrapment efficiency (EE %), and long-term stability. The *in vitro* drug release and *in vivo* skin penetration were evaluated using dialysis bag diffusion and Sprague Dawley (SD) rats, respectively. Cytotoxicity and protecting effects were assessed by AlamarBlue® assay, ROS level by DCFH-DA, and tyrosinase activity by L-DOPA assay, measuring the absorbance at 470 nm. The selected formulations had optimal surface characterizations, including Z-average size, PDI, and Zeta potential ranging from 125 to 207 nm, 0.09–0.22, and −7 to −24, respectively. They also exhibited physiochemical stability for up to 6 months and EE% above 80 %. The lipids ratio and co-Q10 amount as variable factors significantly affected particle size and zeta potential but were insignificant on PDI. The *in vitro* release diagram showed that Q10-NLC/SLN revealed a fast release during the first 8 h and prolonged release afterward. The *in vivo* skin permeation revealed a higher accumulative uptake of co-Q10 in the skin for Q10-NLC/SLN compared to Q10 emulsions. Both selected Q10-NLC and Q10-SLN could reduce intracellular ROS after exposure to H_2O_2. The Q10-NLC was found to be more potent for inhibiting the tyrosinase activity compared to O10-SLN. The results suggest that the new formulations are promising carriers for topical delivery of co-Q10 as an anti-aging and skin-whitening agent.

1. Introduction

There are several theories for the aging process. The oxidative theory activates reactive oxygen species (ROS), which is the most common in the public mind [1]. It could be more comprehensible considering that most of the lipids in the stratum corneum are unsaturated and, therefore, susceptible to free radical damage [2]. So, dermal anti-aging product formulations use exogenous antioxidants such as vitamins, polyphenols, and flavonoids that our bodies can produce [3]. External antioxidants catalytically remove

* Corresponding author. Nanotechnology Research Center, Pharmaceutical Technology Institute, Mashhad University of Medical Sciences, Mashhad, Iran.
E-mail address: Golmohamadzadehsh@mums.ac.ir (S. Golmohammadzadeh).

https://doi.org/10.1016/j.heliyon.2024.e31429
Received 11 May 2024; Accepted 15 May 2024
Available online 22 May 2024

oxidants, such as superoxide dismutase, superoxide reductase, catalase, and glutathione peroxidase. Unfortunately, enzymes like catalase and superoxide dismutase become unstable in emulsions due to their sensitivity to UV light, oxygen, and heat [3]. Coenzyme Q10 (co-Q10) or ubiquinone is the only lipid-soluble antioxidant synthesized in human and animal cells [4,5]. Co-Q10 is able to transport electrons between its three chemical forms: a wholly reduced form (ubiquinol), a semi-oxidized intermediate free radical (semiquinone), and a completely oxidized (ubiquinone) [6]. The main duty of co-Q10 is in the mitochondrial electron transport chain (ETC) [7]. Therefore, higher levels of co-Q10 could be found in the cells in tissues with more mitochondrial content and higher metabolic rates (heart, muscle, liver, and kidney) [7]. Co-Q10 prevents lipid peroxidation and protects tissues against ROS [8]. As an antioxidant and skin strengthener, it can be found in the epidermis 10 times more than the dermis because it is directly exposed to environmental factors such as UV radiation, which is prone to the depletion of skin antioxidants, including co-Q10 [9]. Co-Q10 can protect the skin matrix and fibroblasts and increase hyaluronic acid and collagen in the skin [10].

According to the reports, co-Q10 can also reduce melanin synthesis by inhibiting tyrosinase activity [11,12]. CoQ10 downregulates melanin synthesis through the suppression of MITF expressing and cAMP-mediated CREB signaling cascades [11]. Compared to other melanin synthesis inhibitors, which are used in skin whitening products like arbutin, kojic acid, hydroquinone, corticosteroids, and Hg, co-Q10 is a natural agent with no side effects like dermatitis, steroid ache, exogenous ochronosis, and nephrotic syndrome.

Unfortunately, the amount of co-Q10 decreases due to the reduction of its biosynthesis with aging. Topical administration of co-Q10-containing products prevents aging by reducing oxidation levels and wrinkle depth [9]. High molecular weight (863.36 g/mol), chemical instability (instability against light radiation), high lipophilicity (log $P > 10$), and low solubility in water (0.193 μg/ml) [13,14] are limitations for topical use of co-Q10. Research proved that using nano-drug delivery systems (NDDS) such as liposomes [15,16], nanoemulsions (NE) [17,18], solid lipid nanoparticles (SLN) [19,20], and nanostructured lipid carriers (NLC) [21] can overcome and provide good skin penetration for coenzyme Q10 [22]. Research findings about Q10-NDDS indicate that liposomes excel in reducing ROS accumulation and promoting cell proliferation, NLCs provide enhanced skin penetration and superior antioxidant properties, while SLNs offer high drug entrapment efficiency but may lack the protective effects against ROS accumulation seen with liposomes [23–25]. Each of these lipid-based delivery systems presents unique advantages in co-Q10 skin delivery [25].

NLCs, a variation of SLNs, combine solid and liquid lipids to inhibit complete crystallization, resulting in a more amorphous structure. This matrix modification increases the drug-holding capacity and porosity, thereby enhancing the stability and controlled release potential of co-Q10 [23]. The pioneering Cutanova Nanorepair Q10 cream, the first cosmetical product from NLC containing co-Q10, was introduced by Dr. Rimpler GmbH of Germany in 2005 [26]. Subsequent research has been dedicated to enhancing the formulation of NLC/SLN for efficient co-Q10 delivery in topical drug administration [25,27,28]. This study focuses on creating optimal formulations for advanced skincare products, aiming to provide the skin with antioxidant and antityrosinase benefits. In our previous study, 35 Q10-NLC formulations were developed to assess the effect of solid lipids and surfactants on surface characteristics and long-term stability [29]. Two formulations, incorporating compritol and tripalmitin as solid lipids, were identified as promising candidates [29]. Building upon this groundwork, herein we aimed to evaluate the effect of liquid lipid ratio and co-Q10 amount on the properties of new Q10-NLC/SLN (F1–F18) followed by surface characterization, long-term stability, entrapment efficiency, modulation of ROS level, inhibition of melanin synthesis, and antityrosinase activity measurements.

2. Materials and methods

2.1. Materials

Coenzyme Q10 was prepared from Tinab Shimi Khavarmianeh (Mashhad, Iran, pharmaceutical grade). Glyceryl behenate (Compritol® 888 ATO) was gifted from Gattefossé (Pvt. Ltd. France). Glyceryl tripalmitate (Tripalmitin) and Methanol were purchased from Fluka (Germany); Tween 80 from Kimyagaran Emrooz (Tehran, Iran); Medium-chain triglyceride (MCT) from Oxin Chemistry Company (Kh. Razavi, Iran); Tetrahydrofuran from CARLO ERBA (Emmendingen, Germany); Dimethyl sulfoxide (DMSO), Span® 80, Phenylmethanesulfonyl fluoride (PMSF), N-acetilcisteína (NAC), l-3,4-dihydroxyphenylalanine (L-DOPA), 2′, 7′-dichlorofluorescein diacetate (DCFH-DA), and kojic acid from Sigma-Aldrich Co. (Deisenhofen Germany), The bicinchoninic acid (BCA), and a protein assay kit, from Pierce Co. (Pierce, Rockford, IL, USA). All chemicals were of analytical grade.

The Dulbecco's Modified Eagle Medium (DMEM) and Fetal Calf Serum (FBS) were prepared from Gibco (Grand Island, New York, USA); Resazurin (AlamarBlue®) from BioSource Invitrogen and doxorubicin (10 mg/5 ml) from Ebewe.

2.2. Preparation of Q10-NLC/SLN

To prepare the co-Q10 loaded NLC/SLN, a mixture of surfactant and lipids as the lipid phase and distilled water as the aquas phase were heated to about 10 °C above the lipids' melting point, co-Q10 was added to the lipid phase at the last minute before mixing the two phases. The mixture was homogenized by Ultra-Turrex (Heidolph DIAK) at 5 °C above the melting point of solid lipid in four consecutive steps: 1 min at 22000 rpm, 1 min at 24000 rpm, 1 min at 26000 rpm, and 10 s at 28000 rpm. Afterward, the desired pre-emulsion was sonicated using a sonicator probe (Bransonic, USA) in 7 cycles of 60 s with a rest time of 15 s between each cycle. Finally, the suspension was allowed to cool naturally at room temperature over 24 h, facilitating the formation of NLC/SLN without the need for external cooling or stirring [30,31].

To prepare the Q10-emulsion NLC/SLN formulations, two phases containing the same ingredients were mixed by shaking.

2.3. Entrapment efficiency (EE)%

The separation of free co-Q10 from the NLC/SLN mixture was done by the ultrafiltration method. The centrifugal filter tubes (Amicon ultra®, Millipore, USA) with a molecular weight cutoff 30 kDa were used. About 2 ml Q10-NLC/SLN was transferred to the filter tube and centrifuged at 13000 rpm for 10 min at 4 °C by refrigerated centrifuge (*Sigma 3*–30K, Sigma Laborzentrifugen GmbH, Germany). High-performance liquid chromatography (HPLC; Shimadzu, Japan) equipped with a Lichrospher C8 column (5 Am, 4.6 mm ID25 cm, Hanbag, Dalian, China) was applied to analyze the co-Q10 amount. The isocratic method was used, including the mixture of methanol/tetrahydrofuran 95:5 (V/V) as the mobile phase with 1 ml min^{-1} flow rate, and the UV wavelength was 275 nm. The sample injection was repeated three times. A ten-point standard curve was drawn according to the concentration range (0.0012–2 mg/ml) and area under the curve (AUC) average using Excel 2016 software. The limit of detection (LOD) and limit of quantitation (LOQ) were calculated by the LINEST function.

Both direct and indirect methods were assessed, and considering the obtained LOD and LOQ, the encapsulation efficiency % was performed using a direct method reported in our previous study [29].

The methods for characterization and Physicochemical Stability of the Q10-NLC/SLN and also cell culture are defined in the supplementary file.

2.4. In vitro release study

The Q10-NLC/SLN suspension and Q10-emulsion *In vitro* release were assessed by dialysis bag diffusion with 12 kDa molecular weight cut off (Visking® dialysis tubing, Servia, Greece). About 1 ml of F3 (NLC), F9 (SLN), and Q10-emulsions (prepared using F3 and F9 ingredients) were sealed in dialysis bags and put in 40 ml of a release buffer (5 % w/w tween 80, 20 % w/w tetrahydrofuran, 30 % w/w ethanol, and 45 % w/w phosphate buffer with pH = 7.4) at 37 ± 0.5 °C, with the steering speed of 100 rpm. The analysis test was performed on 2 ml of the buffer at 0.5, 1, 2, 4, 6, 8, 12, and 24 h (the same amount was replaced). The released co-Q10 was measured by the HPLC method, as previously mentioned. The accumulation amount of released co-Q10 at the desired times was obtained by Equation (1) [32].

$$Mn = C_n \times V_t + \sum C(n-1) \times Vs \quad (1)$$

The M_n denotes cumulative drug concentration, C_n symbolizes the observed co-Q10 concentration at times t and zero, V_t is the total release environment volume, $C_{(n-1)}$ is the concentration obtained in the past time, and V_s shows the sample volume removed.

2.5. In vivo skin penetration

This study adheres to ethical guidelines, with the experimental animal ethics approval number being 4001338. Sprague-Dawley (SD) rats weighing between 250 and 300 g were used. The rats were kept in a controlled environment with a 12-h light-dark cycle and had unrestricted access to food and water. To minimize stress, they underwent a one-week acclimatization period. All procedures followed the guidelines established by the Institutional Animal Care and Use Committee (IACUC) to ensure the animals' well-being and minimize discomfort [33]. Two groups of male SD rats (each group containing 8 rats), aged 8 weeks, were used to investigate the co-Q10 skin penetration in NLC and SLN formulations compared to the Q10 emulsions. First, the desired animal was anesthetized with ketamine/xylazine. The rat's back hair was shaved to mark the circles with a diameter of 2 cm, and then 250 μl of Q10-NLC/SLN suspensions, and Q10 emulsions were spread on the desired area. Animals were killed after 12 h in the first group and the second group after 24 h. The skin's surface was cleaned with paper pads soaked in a solvent (methanol/tetrahydrofuran (50:50)) to collect the remaining sample on the skin surface. The paper pads were sonicated in methanol/tetrahydrofuran (50:50) solution for 30 min. Then, 20 μl of the obtained solution was injected into the HPLC device. To determine the penetrated amount of co-Q10, the treated skin parts were immediately separated and torn into pieces. The skin pieces were sonicated in the same solvent for 30 min and stored in a dark and cold environment. After 24 h, the samples were centrifuged at 13000 rpm at 4 °C for 10 min, and 20 μl of the supernatant was injected into the HPLC device.

2.6. Cell viability

A modified AlamarBlue® assay was applied to evaluate the effects of Q10-NLC/SLN formulations and H_2O_2 on cell viability [34]. In this method, viable cells continuously reduce resazurin (non-fluorescent) to resorufin (fluorescence), consequently generating a quantitative measure of viability and cytotoxicity [35]. In summary, cells were seeded (10^4 cells/well) overnight onto flat-bottomed, 96-well culture plates, followed by incubation with various concentrations of Q10-NLC/SLN (3–50 μg/ml) for 24 h. The culture medium was replaced by the new one containing 10 % AlamarBlue® reagent; after 4 h incubation at 37 °C, the absorbance at 600 nm by a Synergy H4 Hybrid Multi-Mode Microplate Reader (BioTek, Winooski, USA) was measured to determine cell viability.

2.7. Cellular ROS level determination

To measure the reactive oxygen species (ROS), 2′, 7′-dichlorofluorescein diacetate (DCFH-DA) was applied. About 10^4 of B16F10 melanoma cells were cultured in a 96-well plate and treated with prepared blank and Q10-NLC/SLN (0–50 μg/ml) and N-acetyl

cysteine (NAC) as a positive control [36] for 24 h (3 repetitions were considered for each concentration), followed by treating DCFH-DA (10 μM). The cells were exposed to 10 mM H_2O_2 at 37 °C for 2 h. Hydrogen peroxide can oxidize DCFH to DCF as a very high fluorescence product. Considering the DCF fluorescence intensities, intracellular ROS level was recorded using a fluorescent Microplate Reader (VICTOR X5, PerkinElmer, USA) at the excitation wavelength of 485 nm and emission wavelength of 530 nm [37].

2.8. Melanin quantification

About 10^5 melanoma cells were cultured in each well of 12 well plates and treated with Q10-NLC/SLN at a concentration of 50 μM for 24 h. Then, they were floated by trypsinization and washed with PBS, then, NaOH at a concentration of 2 M was added and and were incubated at 100 °C for 30 min. After incubation at 60 °C for 2 h, the melanin content in treated cells was measured at 405 nm [38–41].

2.9. Cellular tyrosinase activity assay

10^5 B16F10 cells were seeded in each well of 12 well plates overnight and then treated with Q10-NLC/SLN at a concentration of 50 μM for 24 h. Afterward, cells were transferred to microtubes. Then, centrifuged at 1000 rpm for 5 min, the cell plate was washed with PBS. 100 μL lysing buffer containing 0.1 mM phenylmethylsulfonyl fluoride, 1 % Triton x-100, and 100 mM sodium phosphate buffer at pH 6.8 was added to each microtube. Cells were lysed by freeze-thaw protocol, and PMSF was renewed every 30 min (considering its average half-life).

Samples were centrifuged at 10000 rpm for 20 min at 4 °C temperature. About 100 μl of the supernatant solution along with 100 μl of L-Dopa (5 mM) were transferred to each well of a 96-well microplate and incubated for 2 h at 37 °C away from the light. The absorbance was measured at 475 nm [42]. The protein contents were quantified using a BCA assay [43], incubated at 37 °C for 1h, and the absorbance was measured at 545 nm.

Table 1
Preparations and surface characteristics of Q10-loaded NLC/SLN (F1–F18).

Formulation	Solid lipid type	Solid lipid (%)	MCT Oil (%)	co-Q10 (%)	Tween80 (%)	Span80 (%)	Z-Average size (nm) ± SD	PDI ± SD	Zeta Potential (mV) ± SD
F1	Tripalmtin	3.5	1.5	0.25	4	1	134.9 ± 2.45	0.143 ± 0.004	−11.3 ± 0.37
F2		3.5	1.5	0.5			130.3 ± 3.19	0.171 ± 0.002	−12.6 ± 0.29
F3		3.5	1.5	1			178.9 ± 3.34	0.094 ± 0.003	−11.4 ± 0.70
F4		4.5	0.5	0.25			140.6 ± 3.01	0.117 ± 0.007	−11.0 ± 0.41
F5		4.5	0.5	0.5			207.4 ± 0.86	0.128 ± 0.005	−19.5 ± 0.29
F6		4.5	0.5	1			159.7 ± 1.08	0.176 ± 0.004	−17.8 ± 2.36
F7		5	0	0.25			125.7 ± 2.84	0.168 ± 0.004	−11.5 ± 0.45
F8		5	0	0.5			246.3 ± 3.19	0.191 ± 0.002	−15.0 ± 0.42
F9		5	0	1			192.4 ± 4.50	0.191 ± 0.008	−20.9 ± 1.03
F10	Compritrol	3.5	1.5	0.25	4	1	154.7 ± 5.43	0.165 ± 0.017	−10.9 ± 1.88
F11		3.5	1.5	0.5			172.1 ± 0.77	0.156 ± 0.004	−18.2 ± 0.32
F12		3.5	1.5	1			173.2 ± 2.19	0.117 ± 0.001	−19.2 ± 1.59
F13		4.5	0.5	0.25			184.2 ± 2.44	0.212 ± 0.003	−6.7 ± 0.57
F14		4.5	0.5	0.5			186.6 ± 3.10	0.229 ± 0.008	−15.1 ± 0.81
F15		4.5	0.5	1			199.7 ± 3.78	0.178 ± 0.007	−16.5 ± 0.94
F16		5	0	0.25			142.0 ± 5.64	0.222 ± 0.003	−7.4 ± 1.76
F17		5	0	0.5			206.5 ± 2.95	0.25 ± 0.004	−15.0 ± 0.34
F18		5	0	1			197.3 ± 3.42	0.19 ± 0.007	−24.3 ± 1.02

2.10. Data analysis

Statistical analysis was done by One-way ANOVA (GraphPad Prism 9.0; GraphPad Software, Inc., USA). The effect of variable factors on the particle size, PDI, and zeta potential were investigated by Two-way ANOVA. *P*-values less than 0.05 were considered statistically significant.

3. RESULTS

3.1. Physicochemical characterization of the Q10-NLC

The PCS results for freshly produced Q10-NLC/SLN are reported in Table 1. The Z-average values ranged from 125 nm (F6) to 207 nm (F25). Also, the PDI values ranged from 0.09 to 0.22, and the zeta potential in negative values ranged from −7 to −24 (Table 1). Statistical analysis using two-way ANOVA was performed. The effect of the liquid lipid ratio and co-Q10 amount factors on surface characteristic results were determined in two groups of NLC/SLN formulations that differ in solid lipid. Statistical analysis showed that the mentioned factors' effect and interaction on Z-Average size and Zeta Potential were significant (***$p < 0.0001$). In the case of PDI, the desired factors showed insignificant effect ($P > 0.05$). The percentage of variance determined by each factor is reported in (Table S1 in the supplementary file).

3.2. TEM and SEM analysis

The formulation F3 was selected for microscopic morphology analysis. The Z-average size was estimated at 178 nm. The TEM and SEM images indicated that the Q10-NLC formulation (F3) size was 100–200 nm.

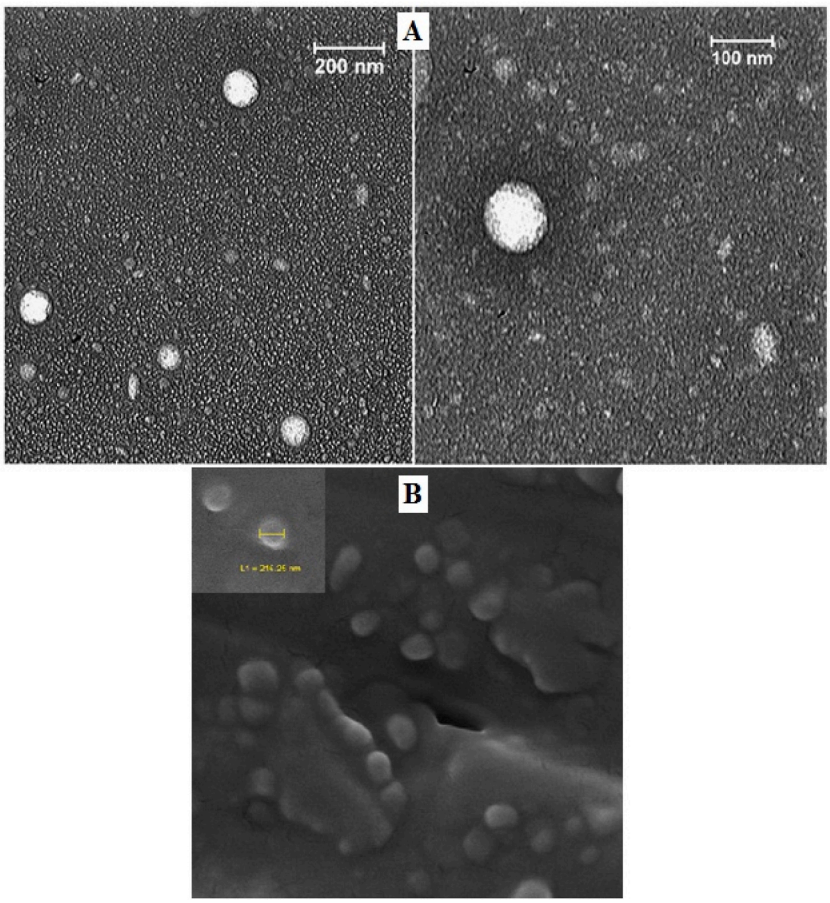

Fig. 1. TEM (A) and SEM (B) images of Q10 loaded NLC (F3).

3.3. Differential Scanning Calorimetry (DSC)

The DSC diagrams for F3, F9, F12, and F18 formulations and their solid ingredients are shown in Fig. 2Fig. 1). The melting peak at 51, 64, and 70 °C belongs to co-Q10, tripalmitin, and compritol, respectively, and were in accordance with their melting points. The bulk lipid melting points decreased after becoming NLC/SLN formulations, and encapsulation of co-Q10 in the lipid matrix disappeared the peak at 51 °C.

3.4. Fourier transform infrared (FT-IR)

The FT-IR spectrum of lipids, co-Q10, and freeze-dried Q10-NLC/SLN formulations, including F1 and F6 in the 400-4000 cm^{-1} range, is shown in Fig. 2. The C–H stretching, C═O stretching, C═C stretching, and C–O stretching of co-Q10 were displayed at 2944, 1648, 1610, and 1203 cm^{-1}, respectively. The FT-IR spectra of the lipids revealed the absorption of carbonyl group stretching for tripalmitin at 1726 and 1736, compritol at 1739, and MCT oil at 1745. The FT-IR spectrum of Q10-NLC/SLN formulations did not display a new peak. The NLC/SLN formulations spectrum shows no significant shift, indicating no chemical reaction.

3.5. Entrapment efficiency (EE%)

The calibration curve was drawn (Figure S1 in the supplementary file), and linear response (R2 = 0.9988), LOD ≥0.05 mg/ml, and LOQ ≥0.15 mg/ml were assessed. The co-Q10 concentrations were found to be less than LOQ in the indirect method, so the direct method was applied to the EE% measurement. The Q10-NLC/SLN formulations containing the highest amount of co-Q10 (1 %); F3, F6, F9, F12, F15, and F18 were selected to investigat the co-Q10 EE%. The results show that co-Q10 was highly encapsulated in selected formulations, as reported in Table 2. EE% has risen by reducing the liquid-to-solid lipid ratio in lipid-content-constant formulations. In summary, more encapsulation was observed in SLN formulations than in NLC, regardless of lipid type. Also, the EE% was measured for F3, F9, F12, and F18 after 6 months. The results showed a slight decrease in EE%, indicating chemical stability over time.

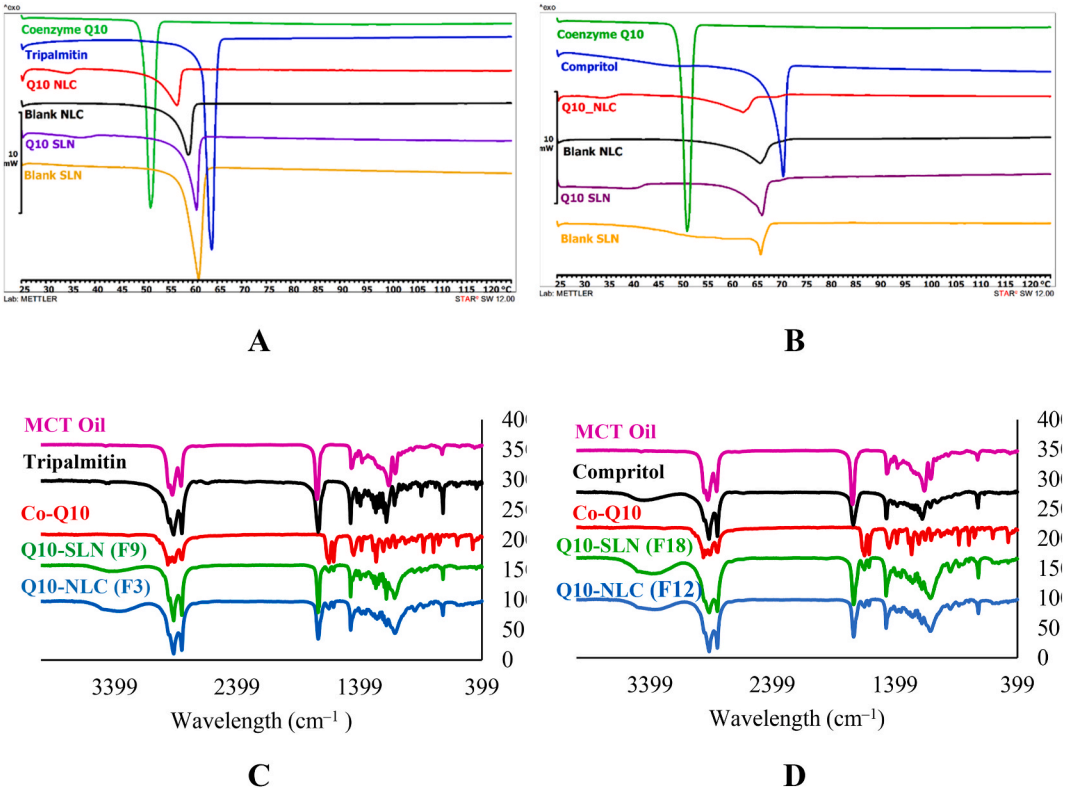

Fig. 2. The obtained DSC curves for freeze-dried blank and Q10 loaded NLC/SLN, co-Q10, and solid lipids. **A:** diagram belongs to F3 and F9 formulations, and **B:** diagram belongs to F12 and F18, respectively. The FT-IR spectra of freeze-dried Q10-NLC/SLN, co-Q10, and lipids in the 4000–400 cm–1 range. **C:** displays the FT-IR spectra for F3 and F9, and **D:** shows the FT-IR spectra for F12 and F18 formulations.

Table 2
The EE% of formulations containing 1 % co-Q10 after preparation and after 6 months.

Formulation	Solid: liquid lipids	Entrapment efficiency% (Fresh)	Entrapment efficiency% (after 6 months)
F3	70:30	81.0 ± 1.21	68.3 ± 2.43
F6	85:15	87.6 ± 2.36	–
F9	100:0	96.3 ± 2.14	88.2 ± 2.72
F12	75:30	80.4 ± 3.23	68.6 ± 2.61
F15	85:15	88.6 ± 1.98	–
F18	100:0	97.9 ± 2.47	85.7 ± 1.84

3.6. Physiochemical stability

The formulations containing 1 % co-Q10 were selected for the physicochemical stability study. The relevant Z-average size, PDI, and Zeta Potential were evaluated at 4, 25, and 40 °C temperatures after 1, 3, and 6 months (Table S2 in the supplementary file).

3.7. In vitro release study

The results of Q10-NLC/SLN compared to Q10 emulsion *in vitro* release are shown in Fig. 3A. Tween 80, ethanol, and tetrahydrofuran were added to the release media to improve the solubility of the co-Q10 in the aquatic environment. None of the ingredients interfere with co-Q10 analysis in HPLC at 275 nm.

3.8. In vivo skin permeation study

The amount of co-Q10 accumulated in the skin and remained on the skin epidermis for F3 (NLC), F9 (SLN), and Q10-emulsions is shown in Fig. 3B. The results revealed that Q10-NLC and Q10-SLN increased the accumulative amount of co-Q10 in the skin by about 4.5 and 6.5 times more than Q10 emulsions after 24 h. The cumulative amount of co-Q10 in the skin for Q10-SLN was higher than NLC.

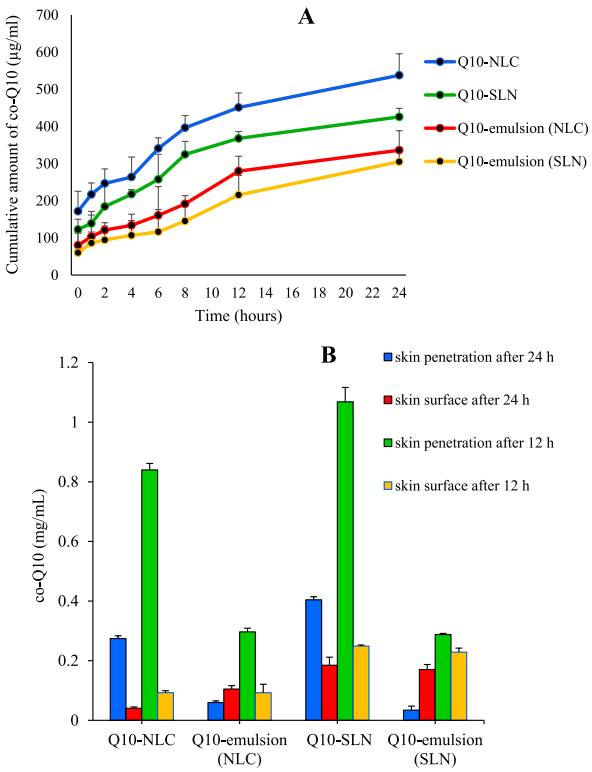

Fig. 3. A: Cumulative amount of released co-Q10 from Q10-NLC, Q10-SLN, and Q10-emulsions versus time. Results are mean ± SEM (n = 3). **B:** The amount of co-Q10 remaining on the skin's surface and accumulated in the skin 12 and 24 h after using Q10-NLC, Q10-SLN, and Q10-emulsion. Results are mean ± SEM (n = 3).

3.9. Cell viability

The *in vitro* antiproliferative activity of Q10-NLC/SLN formulations and H_2O_2 against mouse melanoma cells (B16F10) was evaluated by AlamarBlue® assay. The Q10-NLC, Q10-SLN, free co-Q10, and blank-NLC/SLN formulations for 24 h did not induce toxicity in B16F10 cells at 12–50 μg/ml compared to the control group (Figure S2 (A) in the supplementary file). According to the results, H_2O_2 (10 mM) reduced the viability, while pretreatment with Q10-NLC/SLN (12–50 μg/ml) protected the B16F10 cells (Figure S2 (B) in the supplementary file). Also, this protective effect for drug-free NLC/SLN formulations (F3, F9, F12, and F18) was evaluated, and nonsignificant results were observed (data were not reported).

3.10. The effect on cellular ROS level

The DCF absorbance was measured after treatment with H_2O_2 to understand whether prepared formulations decrease the amount of ROS in melanoma B16F10 cells. The results showed that intracellular ROS levels increased significantly after treatment with H_2O_2. However, cell pretreatment with Q10-NLC/SLN suppressed ROS production and protected against H_2O_2-induced cytotoxicity (Fig. 4A&B). The free co-Q10 showed a lower protective effect compared to Q10-NLC/SLN formulations. In addition, Q10-NLC/SLN reduced the amount of ROS more than the blank NLC/SLN (Fig. 3S in the supplementary file). In formulations consisting of tripalmitin, SLN was more potent than NLC. The prepared formulations from compritol were significantly more successful in reducing ROS levels and no significant difference was observed between NLC and SLN in the compritol group.

3.11. The effect on melanin production

The melanin level diagram in the treated melanoma cells (Fig. 5A) shows that melanin production decreased in the treated cells with Q10-NLC/SLN compared to the non-treated cells. Both Q10-NLCs were more potent than Q10-SLN formulations in decreasing the melanin level in B16F10 cells.

3.12. Antityrosinase activity

Tyrosinase activity in B16F10 cells after treatment with Q10-NLC/SLN compared with their controls pictured in Fig. 5B. According to the results, free co-Q10 and Q10-SLN had no significant effect on tyrosinase enzyme activity. However, both Q10-NLC formulations made of tripalmitin and compritol effectively decreased the activity of the tyrosinase enzyme more than drug-free NLC/SLN formulations (F3, F9, F12, and F18). Each sample contained 1.1 ± 0.1 mg/ml protein.

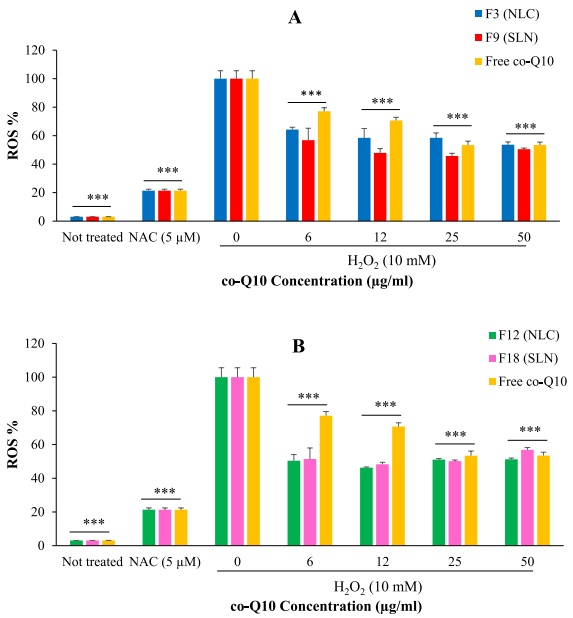

Fig. 4. NLC/SLN formulations of tripalmitin (**A**) and compritol (**B**) suppressed ROS produced by H_2O_2 in B16F10 cells. Cells were pretreated with different concentrations of co-Q10 (6–50 μg/ml) loaded NLC/SLN formulations for 24 h, then treated with H_2O_2 (10 μM) for the next 2 h. Results are mean ± SEM (n = 3). The asterisks indicate statistical differences obtained compared to their controls (treatment with H_2O_2) shown in the figure as *P < 0.05, **P < 0.01, and ***P < 0.001.

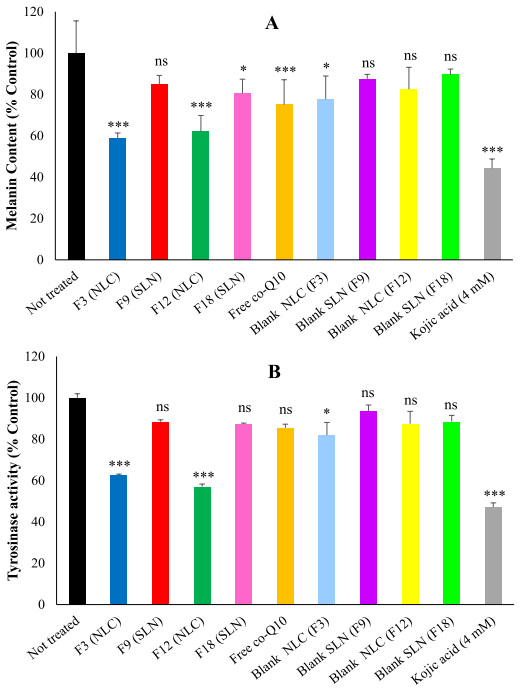

Fig. 5. B16F10 cells were treated with co-Q10 (50 μg/ml) loaded NLC/SLN and kojic acid (4 μM) as a positive control for 24 h to compare the melanin content (**C**), and tyrosinase activity (**D**). D: Results are mean ± SEM (n = 3). The asterisks indicate statistical differences obtained compared to their control (Not treated) shown as *P < 0.05, **P < 0.01, and ***P < 0.001.

4. Discussion

The NLC/SLN are sub-micron colloidal carriers of physiological lipids dispersed in water or an aqueous surfactant solution [44]. The highly ordered crystallinity in the SLN structure decreases drug loading and is limited to the solubility of the drug in lipid melt [44]. Research revealed that MCT oil, containing short carbon chain lengths, is used extensively as a liquid lipid in NLC formulations, increasing drug loading capacity and release rates [45]. So, we aimed to investigate the effect of the MCT oil to solid lipids ratio (0–30 %) on the Q10-NLC/SLN properties. According to the results of our previous study, tripalmitin and compritol as solid lipids were chosen [29]. For further investigation on the role of the co-Q10 content on formulation characteristics, F1–F18 were prepared, and characterized. Then *In vitro* release, skin penetration, antioxidant and antityrosinase activities of the selected formulations were evaluated.

Particle size diameter is one of the critical properties for a nanocarrier to become a promising dermal agent. Many factors, such as preparation conditions, the type and ratio of ingredients, and the active compound amount are involved in determining the particle size of the NLC/SLN formulations [46]. So herein, we evaluated the effect of the lipids ratio and the variety of co-Q10 amounts on Q10-loaded NLC/SLN properties. Surface characteristic results revealed that formulations prepared using tripalmitin (F1-9) and compritol (F10-18) showed desirable particle sizes of less than 210 nm and stability for more than 6 months. According to the results in Table 1 and Table S1, variety in lipid ratio did not affect the particle size significantly. However, the particle size correlated directly to the co-Q10 amount.

The polydispersity index (PDI), is defined as a measure of size dispersion and varies from 0 to 1. The values of <0.35, belong to the favorable distribution of NLC/SLN formulation, which provides long-term stability [47]. The PDI value for F1 to F18 was <0.22. The statistical analysis results showed that the variety in lipid ratio and coenzyme amount did not play an effective role in this factor.

Zeta potential as a physical property indicates the physical stability of colloidal dispersions [48]. In all Q10-NLC/SLN with different lipid ratios, the lowest zeta potential belonged to the formulations containing the lowest amount of co-Q10. So, the existence of a direct relationship between them can be inferred.

Surface modification of F3 evaluated by TEM and SEM. In the obtained images, nano-sized particles approximately <200 nm had a spherical shape, and good dispersity was observed. The difference between particle size in SEM and TEM is convincing by considering the effect of photography conditions on the particle size [49].

The NLC/SLN formulations' melting points decreased compared to bulk lipid melting points caused by the entry of other small molecules like active ingredients and liquid lipids into the lipid matrix [50]. So, this reduction was more for NLC than SLN formulations due to the introduction of liquid oil into the lipid matrix leads to an increase in irregularity in the NLC structure [41,51]. For example, the melting point of tripalmitin decreased from 64 °C to 59 °C and 61 °C for NLC and SLN, respectively. The amorphous characteristic of co-Q10 in the lipid matrix led to the disappearance of the co-Q10 peak at 50.8 °C. The tripalmitin and compritol enthalpy was higher

than the blank NLC/SLN (175.39 J/g, 112.03 J/g in lipid bulk versus 61.98 J/g, 51.41 J/g in blank NLC/SLN respectively), indicating the lipids' structures in the NLC/SLN formulations loss the crystallinity [50,52–54].

The FT-IR spectra provide information on the involvement of functional groups in chemical reactions and changing chemical structures [55]. In the FT-IR spectra of Q10-NLC/SLN (Fig. 2C&D), the absorption bands for carbonyl groups in the lipids and co-Q10 as the functional groups in FT-IR spectroscopy did not shift significantly, Moreover, the FT-IR spectra of Q10-NLC/SLN did not reveal new peaks compared to co-Q10 and the lipids spectra. It indicated preserving the co-Q10 chemical structure in NLC/SLN formulations and was only captured in the lipid matrix [29,56,57].

The EE % results revealed high co-Q10 encapsulation in the selected Q10-NLC/SLN as ordered: F9 and F18 > F6 and F15 > F3 and F12. Therefore, the EE % was higher for SLN formulations containing a maximum amount of solid lipid at the same lipid content. It is expected that high lipophilicity (log P > 10) of co-Q10 leads to more intensity in interaction with the solid lipids, which have bigger hydrocarbon structures than liquid lipids with short carbon chain lengths.

The physiochemical stability of Q10-NLC/SLN formulations refers to their ability to maintain their properties and characteristics under various storage conditions over a certain period. The reported factors affecting the physiochemical stability of Q10-NLC/SLN formulations included oil content in Q10-NLC [24,58], the type and amount of surfactants [24,29], and the effect of solid lipids [29]. In our previous research, we investigated the effect of solid lipid and surfactant types on the long-term stability of Q10-NLCs. herein, To develop our research in this field, we have prepared new Q10-NLC/SLN formulations F1–F18 to evaluate the effect of liquid-to-solid lipid ratio (in the same lipid content) and co-Q10 amount on long-term stability. The obtained results revealed that all formulations F1–F18 showed physiochemical stability at 4, 25, and 40 °C for more than 6 months, and no signs of instability, such as color changes and phase separation were observed. In addition, no significant changes in Z-Average size, PDI, and Zeta potential after 6 months were considered (Table4 in the supplementary material file). Also, F1–F18 formulations The EE% measurement of prepared Q10-NLC/SLN after 6 months confirmed that NLC/SLN are suitable nanocarriers for incorporating co-Q10 to increase chemical stability [19,59,60]. It can be deduced that the two variables factors including the amounts of liquid lipid and co-Q10 do not have a significant effect on the stability results, although the type of solid lipids and surfactants had more effect on the stability of these formulations [29].

The *in vitro* release diagram shows initial fast release in the first 8 h for Q10-NLC/SLN formulations compared to Q10-emulsions was observed, possibly due to the enrichment of Q10 in the outer shell and considering the greater surface area for NLC/SLN particles caused by the particle size diameter of about 100–200 nm compared to the emulsions. The presence of MCT oil in the NLC formulation and smaller particle size may lead to faster release for Q10-NLC than Q10-SLN. Also, slow diffusion of co-Q10 from a solid matrix than the liquid lipids causes a prolonged release after an initial 8 h [61]. Our findings are in agreement with previous studies that have established the impact of particle size on the rate of drug release from nanocarriers. For instance, Wang et al. demonstrated a substantial enhancement in skin penetration for NLC-Q10 compared to an ethanolic co-Q10 solution [62–65], additionally, Zhang et al. reported a more rapid release of co-Q10 from NLCs compared to SLN formulations [64] due to the smaller particle size and the inclusion of MCT oil in NLCs [66].

The skin penetration of NDDS depends on the particle size and their interactions with the skin layers [67]. The *in vivo* skin penetration diagram (Fig. 3B) shows the amount of co-Q10 penetrated through the skin for both Q10-NLC and Q10-SLN after 12 and 24 h was higher than the Q10 emulsion (NLC/SLN), which can be expected according to the average diameter size of about 100–200 nm for Q10-NLC/SLN formulations compared to Q10-emulsions with a particle size of about 800–1000 nm. The amount of remaining co-Q10 on the skin surface for Q10-emulsion was higher than nanocarriers confirming that lipid nanocarriers penetrate better through the stratum corneum [68]. The difference in the accumulative amount of co-Q10 in the skin between Q10-SLN and Q10-NLC could be justified by considering the differences in EE % and release rate. So, Q10-SLN expected higher co-Q10 accumulative amounts than Q10-NLC after 12 and 24 h.

The selected formulations F3, F9, F12, and F18 up to a concentration equal to 0.5 % (V/V) of the culture medium (containing 50 μg/ml co-Q10) did not show significant cytotoxicity against B16F10 cells after 24 h. This aligns with previous research on NLC and SLNs [69,70]. Treatment with H_2O_2 (10 mM) for 2 h reduced viability compared with control. Pretreatment with Q10-NLC/SLN showed a partial protective effect and slightly increased cell viability compared with the H_2O_2 group. There was no significant difference between Q10-NLC and Q10-SLN.

The imbalance between ROS level and antioxidant defense leads to oxidative stress [71]. The antioxidant agents, such as co-Q10, are able to reduce intra-cellular ROS levels and establish the desired balance [71]. Co-Q10 is a lipophilic antioxidant, so encapsulation of co-Q10 by NLC/SLN can improve its distribution in an aqueous medium for *in vitro* studies such as other lipophilic ingredients [12]. The intracellular ROS levels diagram (Fig. 4A&B) shows that free co-Q10 reduces oxidative stress in a dose-dependent manner compared to the H_2O_2 group in B16F10 cells. The Q10-NLC/SLN formulations can prevent ROS increase without cytotoxic effect. Our results showed that Q10-NLC/SLN, as water-soluble co-Q10, can be a promising antioxidant agent and has higher protective activity in comparison with the free form of co-Q10. suggesting that the solid lipids in both formulations have a similar effect on cell uptake. This finding aligns with previous research by Ruktanonchai et al. who reported that both SLN and NLC demonstrated potential as alternative carriers for antioxidants [72,73]. Cellular uptake studies also showed that both NLC and SLN were able to enter Caco-2 intestinal [74], indicating their potential as effective delivery systems for lipophilic antioxidants like co-Q10.

DOPA assay is reported as a tyrosinase activity indicator [12], revealing that both Q10-NLC, regardless of its solid lipid, were more potent in reducing tyrosinase activity than the Q10-SLN formulations. As expected, free co-Q10 showed a weak effect on tyrosinase inhibition. So, according to the results, Q10-NLC could be a candidate for the skin-lightning agent. Results indicated that melanin synthesis was more reduced in cells treated with Q10-NLC/SLN than free co-Q10. This reduction was observed more in Q10-NLC formulation groups than in Q10-SLN treated groups. The melanin content and the tyrosinase inhibition results are consistent and

confirm the decrease in melanin synthesis through the mechanism of tyrosinase inhibition.

5. Conclusion

We prepared new Q10-NLC/SLN formulations (F1–F18) to investigate the effect of lipid ratio and concentration of co-Q10 on the characteristic properties of the nanoparticles. These variable factors significantly affected particle size and zeta potential and were insignificant in PDI. The Q10-NLC/SLN showed desired surface characterization, physiochemical stability, and high EE%. Increasing the solid-to-liquid lipid ratio in the lipid content of NLCs led to an increase in EE % and reached the maximum values in SLNs. New Q10-NLC/SLNs showed faster *in vitro* release and increased *in vivo* skin accumulative properties compared to Q10 emulsions. The Q10-SLN was more successful in skin penetration than the Q10-NLC. The Q10-NLC/SLN formulations as promising candidates for anti-aging revealed a reduction in intracellular ROS levels in B10F10 cells. Notably, Q10-NLC formulations decreased melanin production in melanoma cells through tyrosinase inhibition and were more effective than free co-Q10 and Q10-SLN. So, Q10-NLCs are suggested to serve as anti-aging and skin-lightning agents. However, the development of optimal Q10/NLC/SLN formulations for future skincare products is necessitated. Further, *in vivo* studies are recommended to compare the strengths and weaknesses of these formulations, whether NLC or SLN, for delivering co-Q10 and other proposed components to make well-informed decisions regarding the most suitable nanocarrier system for future skincare products.

CRediT authorship contribution statement

Hoda Atapour-Mashhad: Writing – review & editing, Writing – original draft, Validation, Software, Investigation, Formal analysis, Conceptualization. **Zahra Tayarani-Najaran:** Writing – review & editing, Software, Data curation, Conceptualization. **Shiva Golmohammadzadeh:** Writing – review & editing, Visualization, Validation, Supervision, Project administration, Investigation, Funding acquisition, Conceptualization.

Declaration of Competing interest

The authors declare no conflicts of interest, including financial and other relationships.

Acknowledgements

This work was supported by Mashhad University of Medical Sciences, Mashhad, Iran [grant number 4001338].

Appendix A. Supplementary data

Supplementary data to this article can be found online at https://doi.org/10.1016/j.heliyon.2024.e31429.

References

[1] S. Hekimi, How genetic analysis tests theories of animal aging, Nat. Genet. 38 (9) (2006) 985–991.
[2] R.A. Baxter, Anti-aging properties of resveratrol: review and report of a potent new antioxidant skin care formulation, J. Cosmet. Dermatol. 7 (1) (2008) 2–7.
[3] P. Forsmark-Andrée, L. Ernster, Evidence for a protective effect of endogenous ubiquinol against oxidative damage to mitochondrial protein and DNA during lipid peroxidation, Mol Aspects Med 15 (Suppl) (1994) s73–s81.
[4] R.E. Beyer, Inhibition by coenzyme Q of ethanol- and carbon tetrachloride-stimulated lipid peroxidation in vivo and catalyzed by microsomal and mitochondrial systems, Free Radic. Biol. Med. 5 (5–6) (1988) 297–303.
[5] F.M. Gutierrez-Mariscal, et al., Coenzyme Q(10): from bench to clinic in aging diseases, a translational review, Crit. Rev. Food Sci. Nutr. 59 (14) (2019) 2240–2257.
[6] M. Alcázar-Fabra, P. Navas, G. Brea-Calvo, Coenzyme Q biosynthesis and its role in the respiratory chain structure, Biochim. Biophys. Acta 1857 (8) (2016) 1073–1078.
[7] I.P. Barcelos, R.H. Haas, CoQ10 and aging, Biology 8 (2) (2019).
[8] S.S. Perumal, P. Shanthi, P. Sachdanandam, Augmented efficacy of tamoxifen in rat breast tumorigenesis when gavaged along with riboflavin, niacin, and CoQ10: effects on lipid peroxidation and antioxidants in mitochondria, Chem. Biol. Interact. 152 (1) (2005) 49–58.
[9] J.D. Hernández-Camacho, et al., Coenzyme Q(10) Supplementation in aging and Disease, Front. Physiol. 9 (2018) 44.
[10] J. Hojerova, Skin Health Benefits of coenzyme Q10, in: R.R. Watson, S. Zibadi (Eds.), Bioactive Dietary Factors and Plant Extracts in Dermatology, Humana Press, Totowa, NJ, 2013, pp. 197–213.
[11] Y.C. Hseu, et al., The in vitro and in vivo depigmenting activity of Coenzyme Q10 through the down-regulation of α-MSH signaling pathways and induction of Nrf2/ARE-mediated antioxidant genes in UVA-irradiated skin keratinocytes, Biochem. Pharmacol. 164 (2019) 299–310.
[12] M. Zhang, et al., Coenzyme Q(10) enhances dermal elastin expression, inhibits IL-1α production and melanin synthesis in vitro, Int. J. Cosmet. Sci. 34 (3) (2012) 273–279.
[13] N. Rosita, et al., Enhancing skin penetration of epigallocatechin gallate by modifying partition coefficient using reverse micelle method 10 (7) (2019) 409–417.
[14] A. Elaimi, et al., Skin penetration of coenzyme Q10 in nanostructure lipid carriers using olive oil and cetyl palmitate, International Journal of Pharmaceutical and Clinical Research 9 (2017).
[15] C.J. Pastor-Maldonado, et al., Coenzyme Q(10): novel formulations and medical trends, Int. J. Mol. Sci. 21 (22) (2020).
[16] H. Li, F. Chen, Preparation and quality evaluation of coenzyme Q10 long-circulating liposomes, Saudi J. Biol. Sci. 24 (4) (2017) 797–802.
[17] C.J. Pastor-Maldonado, et al., Coenzyme q10: novel formulations and medical trends, Int. J. Mol. Sci. 21 (22) (2020) 8432.
[18] H. Soni, S. Sharma, Current update on nanoemulsion: a review, Sch. Int. J. Anat. Physiol 4 (1) (2021) 6–13.

[19] E.S. Farboud, S.A. Nasrollahi, Z. Tabbakhi, Novel formulation and evaluation of a Q10-loaded solid lipid nanoparticle cream: in vitro and in vivo studies, Int J Nanomedicine 6 (2011) 611–617.
[20] Chaiprateep, S. and P. Naruphontjirakul, Synthesis of Solid Lipid Nanoparticles Containing CoenzymeQ10 and Vitamin E through Hot Homogenization Process.
[21] F. Shoviantari, T. Erawati, W. Soeratri, Coenzyme Q10 nanostructured lipid carriers as an inducer of the skin fibroblast cell and its irritability test in a mice model, J. Basic Clin. Physiol. Pharmacol. 30 (6) (2019).
[22] I.D.L. Souza, V. Saez, C.R.E. Mansur, Lipid nanoparticles containing coenzyme Q10 for topical applications: an overview of their characterization, Colloids Surf. B Biointerfaces 230 (2023) 113491.
[23] E.H. Gokce, et al., A comparative evaluation of coenzyme Q10-loaded liposomes and solid lipid nanoparticles as dermal antioxidant carriers, International journal of nanomedicine (2012) 5109–5117.
[24] V.B. Junyaprasert, et al., Q10-loaded NLC versus nanoemulsions: stability, rheology and in vitro skin permeation, International journal of pharmaceutics 377 (1–2) (2009) 207–214.
[25] I.D.L. de Souza, V. Saez, C.R.E. Mansur, Lipid nanoparticles containing coenzyme Q10 for topical applications: an overview of their characterization, Colloids Surf. B Biointerfaces (2023) 113491.
[26] J. Pardeike, K. Schwabe, R.H. Müller, Influence of nanostructured lipid carriers (NLC) on the physical properties of the Cutanova Nanorepair Q10 cream and the in vivo skin hydration effect, Int J Pharm 396 (1–2) (2010) 166–173.
[27] R. Müller, J. Pardeike, Coenzyme Q10-loaded NLCs: preparation, occlusive properties and penetration enhancement, Pharmaceut. Technol. Eur. 19 (7) (2007).
[28] N.L.D. Aryani, et al., Development, characterization, molecular docking, and in vivo skin penetration of coenzyme Q10 nanostructured lipid carriers using tristearin and stearyl alcohol for dermal delivery, J. Basic Clin. Physiol. Pharmacol. 32 (4) (2021) 517–525.
[29] H. Atapour-Mashhad, et al., Preparation, characterization, and molecular Dynamic Simulation of novel Coenzym Q10 loaded nanostructured lipid carriers, Curr. Pharmaceut. Des. 29 (27) (2023) 2177–2190.
[30] M.S. Vaziri, et al., Preparation and characterization of Undecylenoyl Phenylalanine loaded-nanostructure lipid carriers (NLCs) as a new α-MSH Antagonist and antityrosinase agent, Adv Pharm Bull 13 (2) (2023) 290–300.
[31] Z. Jafarifar, et al., Preparation and characterization of nanostructured lipid carrier (NLC) and nanoemulsion containing vitamin D3, Appl. Biochem. Biotechnol. 194 (2) (2022) 914–929.
[32] S. Chen, et al., Preparation of Coenzyme Q10 nanostructured lipid carriers for epidermal targeting with high-pressure microfluidics technique, Drug development and industrial pharmacy 39 (1) (2013) 20–28.
[33] A.K. Kiani, et al., Ethical considerations regarding animal experimentation, J Prev Med Hyg 63 (2 Suppl 3) (2022) E255–e266.
[34] A. Zaker, et al., Cytotoxic and apoptotic effects of root extract and tanshinones isolated from Perovskiaabrotanoides Kar, Iran J Basic Med Sci 20 (12) (2017) 1377–1384.
[35] M.V. Lancaster, R.D. Fields, Antibiotic and Cytotoxic Drug Susceptibility Assays Using Resazurin and Poising Agents, Google Patents, 1996.
[36] Y.S. Im, Y.K. Ryu, E.Y. Moon, Mouse melanoma cell Migration is dependent on production of reactive oxygen species under Normoxia condition, Biomol Ther (Seoul) 20 (2) (2012) 165–170.
[37] E. Hadipour, Z. Tayarani-Najaran, M. Fereidoni, Vitamin K2 protects PC12 cells against Aβ ((1-42)) and H(2)O(2)-induced apoptosis via p38 MAP kinase pathway, Nutr. Neurosci. 23 (5) (2020) 343–352.
[38] A. Ścieżyńska, et al., A novel and effective method for human Primary skin Melanocytes and metastatic melanoma cell Isolation, Cancers 13 (24) (2021).
[39] C.A. Aya-Bonilla, et al., Isolation and detection of circulating tumour cells from metastatic melanoma patients using a slanted spiral microfluidic device, Oncotarget 8 (40) (2017) 67355.
[40] Z. Tayarani-Najaran, et al., Evaluation of antioxidant and anti-melanogenic activities of different extracts from aerial parts of Nepeta binaludensis Jamzad in murine melanoma B16F10 cells, Iranian journal of basic medical sciences 19 (6) (2016) 662.
[41] S. Eghbali-Feriz, et al., Anti-melanogenesis and anti-tyrosinase properties of Pistacia atlantica subsp. mutica extracts on B16F10 murine melanoma cells, Research in pharmaceutical sciences 13 (6) (2018) 533–545.
[42] S.H. Hashemi-Shahri, et al., ROS-Scavenging and anti-tyrosinase properties of Crocetin on B16F10 murine melanoma cells, Anti Cancer Agents Med. Chem. 18 (7) (2018) 1064–1069.
[43] J.M. Walker, The bicinchoninic acid (BCA) assay for protein quantitation, Methods Mol. Biol. 32 (1994) 5–8.
[44] S. Mukherjee, S. Ray, R.S. Thakur, Solid lipid nanoparticles: a modern formulation approach in drug delivery system, Indian J Pharm Sci 71 (4) (2009) 349–358.
[45] R.H. Müller, et al., Nanostructured lipid carriers (NLC) in cosmetic dermal products, Adv. Drug Deliv. Rev. 59 (6) (2007) 522–530.
[46] W. Mehnert, K. Mäder, Solid lipid nanoparticles: production, characterization and applications, Adv. Drug Deliv. Rev. 64 (2012) 83–101.
[47] K.L. López, et al., Solid lipid nanoparticles (SLN) and nanostructured lipid carriers (NLC) prepared by Microwave and Ultrasound-Assisted synthesis: promising green strategies for the Nanoworld, Pharmaceutics 15 (5) (2023).
[48] F. Tamjidi, et al., Design and characterization of astaxanthin-loaded nanostructured lipid carriers, Innovat. Food Sci. Emerg. Technol. 26 (2014) 366–374.
[49] K. Bhaskar, et al., Development of SLN and NLC enriched hydrogels for transdermal delivery of nitrendipine: in vitro and in vivo characteristics, Drug Dev. Ind. Pharm. 35 (1) (2009) 98–113.
[50] S. Sarhadi, et al., Moisturizing effects of solid lipid nanoparticles (SLN) and nanostructured lipid carriers (NLC) using deionized and magnetized water by in vivo and in vitro methods, Iran J Basic Med Sci 23 (3) (2020) 337–343.
[51] I. Chauhan, et al., Nanostructured lipid carriers: a Groundbreaking approach for transdermal drug delivery, Adv Pharm Bull 10 (2) (2020) 150–165.
[52] M.J. Gomes, et al., Lipid nanoparticles for topical and transdermal application for alopecia treatment: development, physicochemical characterization, and in vitro release and penetration studies, International journal of nanomedicine (2014) 1231–1242.
[53] P. Rahmanian-Devin, et al., Preparation and characterization of solid lipid nanoparticles encapsulated noscapine and evaluation of its protective effects against imiquimod-induced psoriasis-like skin lesions, Biomed. Pharmacother. 168 (2023) 115823.
[54] A. Akhoond Zardini, et al., Production and characterization of nanostructured lipid carriers and solid lipid nanoparticles containing lycopene for food fortification, J. Food Sci. Technol. 55 (1) (2018) 287–298.
[55] S. Ramkar, P.K. Suresh, Finasteride-loaded nano-lipidic carriers for follicular drug delivery: preformulation screening and Box-Behnken experimental design for optimization of variables, Heliyon 8 (8) (2022) e10175.
[56] N.L.D. Aryani, et al., Development, characterization, molecular docking, and in vivo skin penetration of coenzyme Q10 nanostructured lipid carriers using tristearin and stearyl alcohol for dermal delivery, J. Basic Clin. Physiol. Pharmacol. 32 (4) (2021) 517–525.
[57] P.A. Makoni, K. Wa Kasongo, R.B. Walker, Short term stability testing of Efavirenz-loaded solid lipid nanoparticle (SLN) and nanostructured lipid carrier (NLC) dispersions, Pharmaceutics 11 (8) (2019).
[58] J. Wang, et al., Physicochemical characterization, photo-stability and cytotoxicity of coenzyme Q10-loading nanostructured lipid carrier, J. Nanosci. Nanotechnol. 12 (3) (2012) 2136–2148.
[59] A. Dingler, et al., Solid lipid nanoparticles (SLN/Lipopearls)–a pharmaceutical and cosmetic carrier for the application of vitamin E in dermal products, J. Microencapsul. 16 (6) (1999) 751–767.
[60] C. Puglia, et al., Evaluation of alternative strategies to optimize ketorolac transdermal delivery, AAPS PharmSciTech 7 (3) (2006) 64.
[61] S. Chen, et al., Preparation of Coenzyme Q10 nanostructured lipid carriers for epidermal targeting with high-pressure microfluidics technique, Drug Dev. Ind. Pharm. 39 (1) (2013) 20–28.
[62] J.C. Schwarz, et al., Ultra-small NLC for improved dermal delivery of coenyzme Q10, Int J Pharm 447 (1–2) (2013) 213–217.
[63] F. Shoviantari, T. Erawati, W. Soeratri, Skin penetration of coenzyme Q10 in nanostructure lipid carriers using olive oil and cetyl palmitate, Int J Pharm Clin Res 9 (2) (2017) 142–145.
[64] E. Subroto, R. Andoyo, R. Indiarto, Solid lipid nanoparticles: review of the Current research on encapsulation and delivery systems for active and antioxidant compounds, Antioxidants 12 (3) (2023).

[65] E.N. Tessema, et al., Investigation of ex vivo skin penetration of coenzyme Q10 from microemulsions and hydrophilic cream, Skin Pharmacol. Physiol. 33 (6) (2021) 293–299.
[66] S. Khan, et al., Nanostructured lipid carriers: an emerging platform for improving oral bioavailability of lipophilic drugs, Int J Pharm Investig 5 (4) (2015) 182–191.
[67] C. Try, et al., Size dependent skin penetration of nanoparticles in murine and porcine dermatitis models, Eur. J. Pharm. Biopharm. 100 (2016) 101–108.
[68] J. Pardeike, K. Schwabe, R.H. Müller, Influence of nanostructured lipid carriers (NLC) on the physical properties of the Cutanova Nanorepair Q10 cream and the in vivo skin hydration effect, International journal of pharmaceutics 396 (1–2) (2010) 166–173.
[69] T. Guo, et al., Nanostructured lipid carriers for percutaneous administration of alkaloids isolated from Aconitum sinomontanum, J. Nanobiotechnol. 13 (2015) 1–14.
[70] J. Pardeike, A. Hommoss, R.H. Müller, Lipid nanoparticles (SLN, NLC) in cosmetic and pharmaceutical dermal products, International journal of pharmaceutics 366 (1–2) (2009) 170–184.
[71] S.V.E. Silva, et al., Antioxidant effect of coenzyme Q10 in the prevention of oxidative stress in Arsenic-treated CHO-K1 cells and possible Participation of Zinc as a Pro-Oxidant agent, Nutrients 14 (16) (2022).
[72] U. Ruktanonchai, et al., Physicochemical characteristics, cytotoxicity, and antioxidant activity of three lipid nanoparticulate formulations of alpha-lipoic acid, AAPS PharmSciTech 10 (1) (2009) 227–234.
[73] C. Viegas, et al., Solid lipid nanoparticles vs. Nanostructured lipid carriers: a comparative review, Pharmaceutics 15 (6) (2023).
[74] P. Mura, et al., Evaluation and comparison of solid lipid nanoparticles (SLNs) and nanostructured lipid carriers (NLCs) as Vectors to develop Hydrochlorothiazide effective and Safe Pediatric oral liquid formulations, Pharmaceutics 13 (4) (2021).